sLHC Project Note 0016

2010-05-17

margarita.garcia.tudela@cern.ch

Reduction of the beam intensity by means of a sieve for Linac4

Margarita Garcia Tudela, Asen Christov, Alessandra Lombardi

Summary

Different types of beams are needed by the PSB, in particular at Linac4 [1]. Low intensity beam can be obtained using a piece called “sieve” in the Linac to PSB transfer line. The aim of this note is to study the dynamics of the protons, generated after this piece, which could activate the vacuum chamber, up to the end of the line, in order to locate the losses and their level.

1. Introduction

Different types of beams are needed by the PSB, in particular at Linac4 [1]. Low intensity beam can be obtained using a piece called “sieve” in the Linac to PSB transfer line.

A sieve is a plate with holes used to reduce the beam intensity, keeping the transverse emittance. The sieve can be made of graphite or copper, and in the present design has 1731 holes of 1.5mm of diameter to reduce the beam intensity by a factor of 5.

When a bunch traverses this equipment, a fraction of the particles goes through the holes and their energy and charge state remains the same. The rest interacts with the sieve; these are either stopped or they lose significant amount of energy. Moreover in the case of H^- the electrons are stripped from the proton and therefore also the charge state changes. Also other particles as neutrons, electrons, photons, etc are generated in this sieve.

The aim of this note is to study the dynamics of the protons, which could activate the vacuum chamber, up to the end of the line, in order to locate the losses and their level. Therefore, the fate of protons and neutrons along the line is studied for Linac4 at 160 MeV.

The simulations were done with the code PathManager [2]

2. Layout Description

A 150 m transfer line brings the Linac4 beam to the booster. The line joins the present linac2-to booster at the location of LT.BHZ20 bending magnet.

Figure 2.1 shows a Trace3D scheme of that second part of the TL. The sieve will be placed about 6m after BHZ.40 bending magnet, in the BI region.

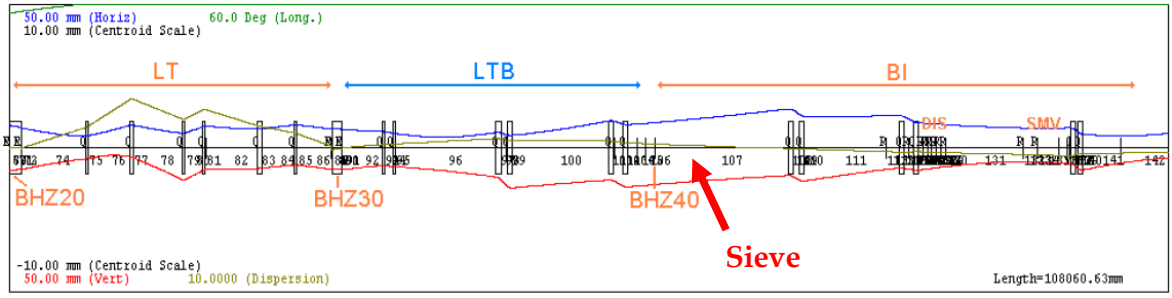

Figure 2.1 Sketch of the Linac2/Linac4 transfer line, common part.

In the BI section the beam is distributed to the four Booster rings by a vertical bending magnet (DVT30), a system of five kicker magnets (DIS), another vertical bend (DVT40) and 3 septum magnets (SMV). The beam enters the distributor with a vertical beam offset and is then sequentially deflected by the combined action of the DIS, DVT40 and SMV into the four separate apertures of the BVT dipole magnet, to achieve the required PSB beam level separation of 360mm between each ring (see the sketch in Fig.2.2). [3]

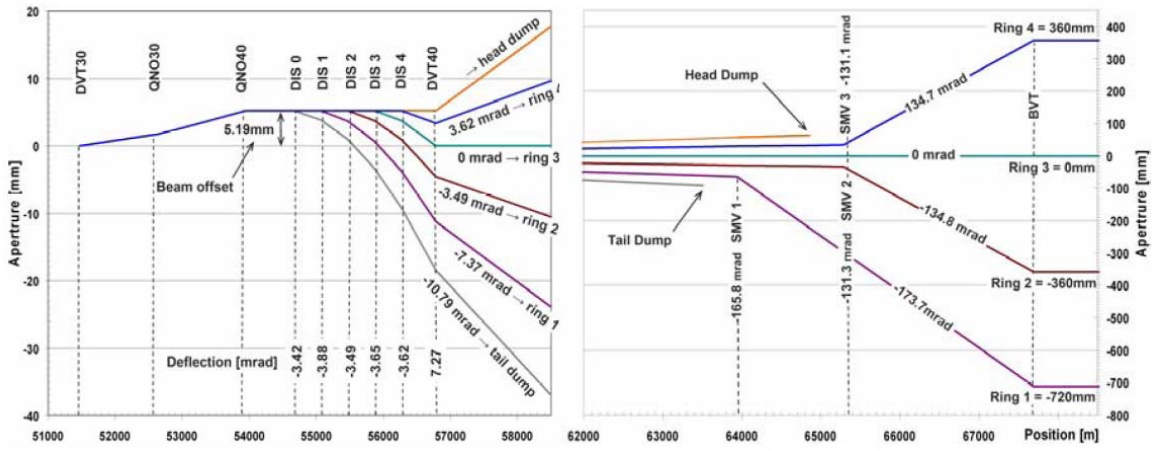

Figure 2.2 Sketch of the beam distribution system into the four PSB rings.

Due to the fact that the H^- beam has 4 different destinations, it is necessary to study each case separately. In the distributor, since the bending angle given by the five kicker magnets to the beam is small, and the aperture is 7 cm radius, the differences in terms of proton losses are small (~mW) and can be neglected. Therefore, in the results presented below, the level of the losses in this area is independent of the H^- destination.

The protons arriving to the septum are mainly lost on the septum input wall and those which enter the septum magnet are bent with the opposite polarity and are lost there. See figure 2.3. In the next sections the losses in the septum are presented depending on the end Booster Ring for H^-.

Therefore, with the present layout, protons and neutrons generated by the sieve are transmitted only to ring 3, where the particles follow a straight path without vertical septum bending.

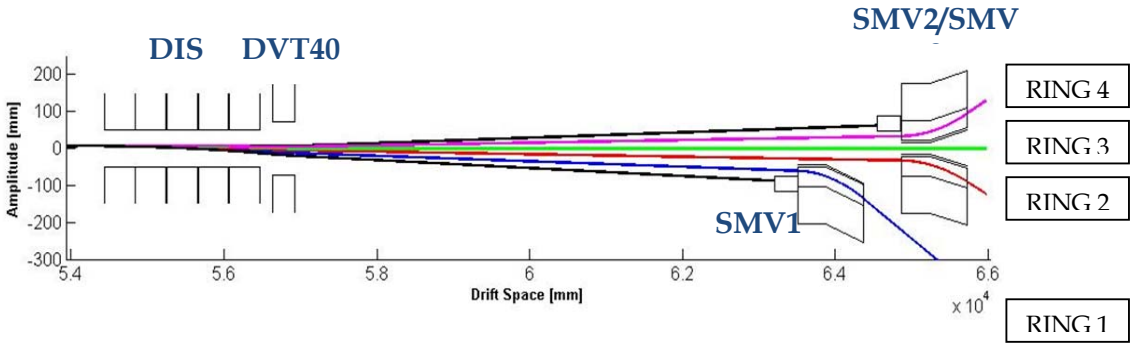

Figure 2.3 Sketch of the beam distribution and physical implementation of the septum magnets.

3. Beam distribution

Beam distributions after the sieve have been calculated with Fluka [4][5].

Before start the simulations and track the particles downstream to the end of the TL, the beam distribution after the sieve is characterized for the four study cases.

Protons generated in the sieve are spread all over the beam pipe. X-y (on the top) and x-x' (on the bottom) phase-spaces are plotted in the figure below, for the H^- beam and H^- plus protons beam. See figure 3.1.

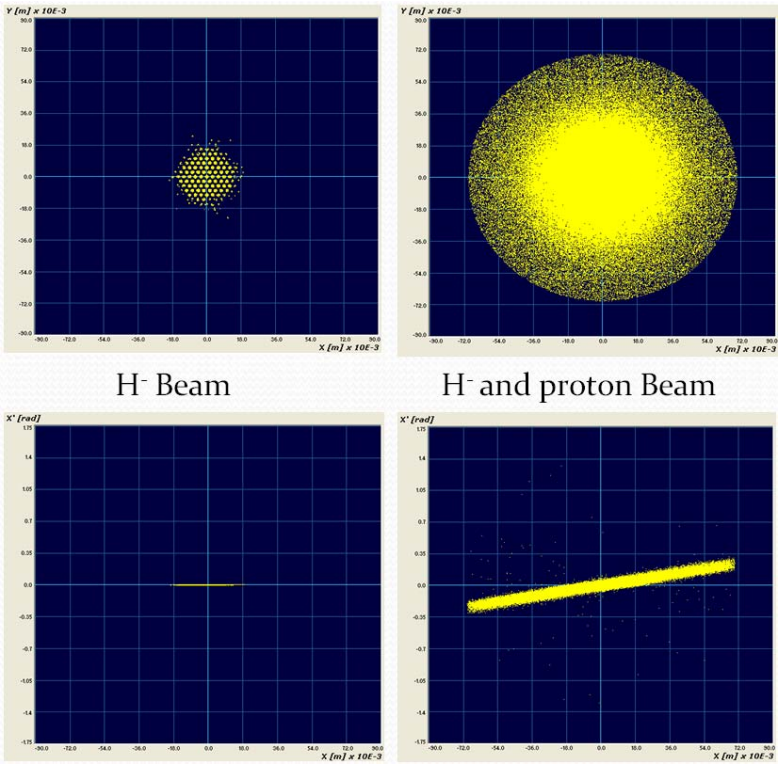

Figure 3.1 Comparison between phase-spaces for H^- and proton beams, after the sieve.

Figure 3.2 shows the incident particle distribution (before the sieve). The plots are in the same scale of the figure above.

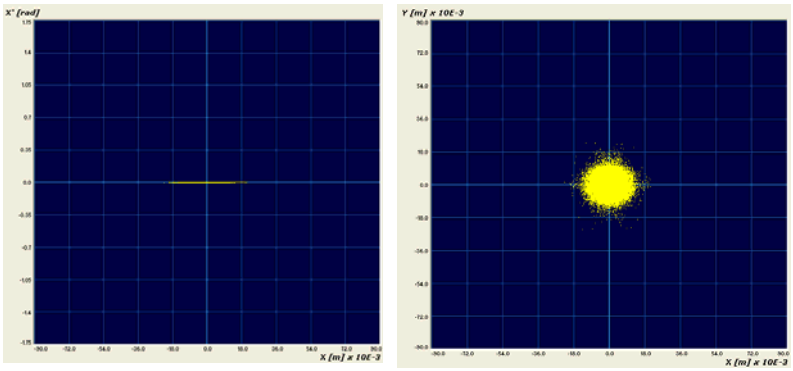

Figure 3.2 Beam distribution at the sieve input.

3.1.- Graphite

For a sieve made of graphite, two different thicknesses are studied, 12 cm and 10.5 cm. Figure 3.1.1 shows the energy distribution of the protons for both lengths, normalized to the number of incident particles.

In the case of Graphite 10.5 cm, a secondary peak appears at low energy, since the thickness of the material is not enough to stop the H^-, so the maximum energy deposition (Bragg peak) is not inside the sieve.

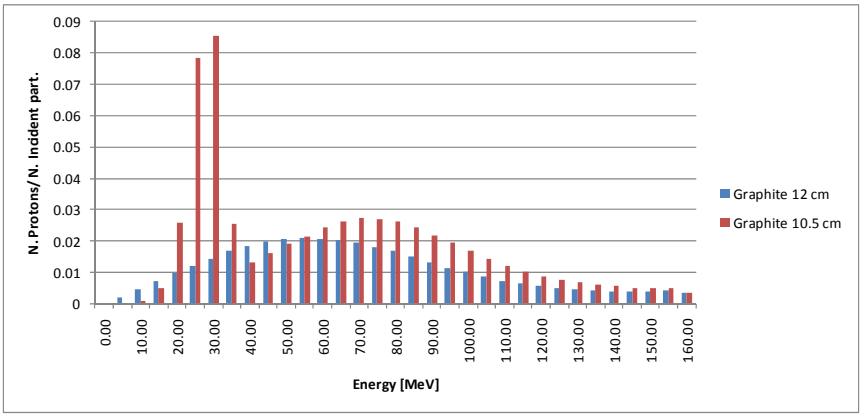

Figure 3.1.1 Proton Energy Distribution after the sieve. Graphite

Figure 3.1.2 shows the energy distribution of H^- for both cases. As it was expected, the H^- particles that pass through the sieve holes without interact with the material keep their incident energy.

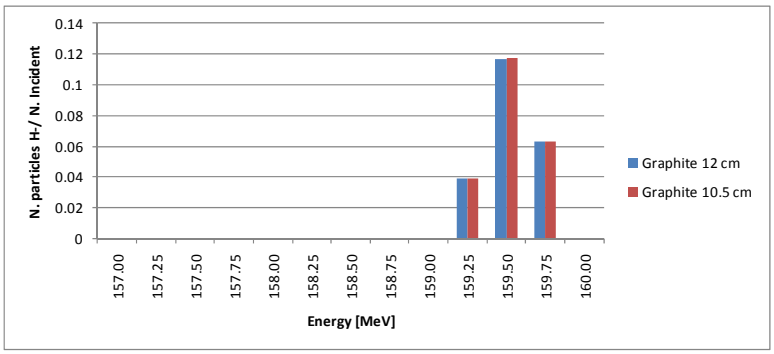

Figure 3.1.2 H^- Energy Distribution after the sieve. Graphite

3.2.- Copper

For a sieve made of copper two different thicknesses are studied, 3 cm and 2.7 cm. Figure 3.2.1 shows the energy distribution of the protons for both lengths.

In the case of Copper 2.7 cm, a secondary peak appears at low energies, since the thickness of the material is not enough to stop the H^-, so the maximum energy deposition (Bragg peak) is not inside the sieve.

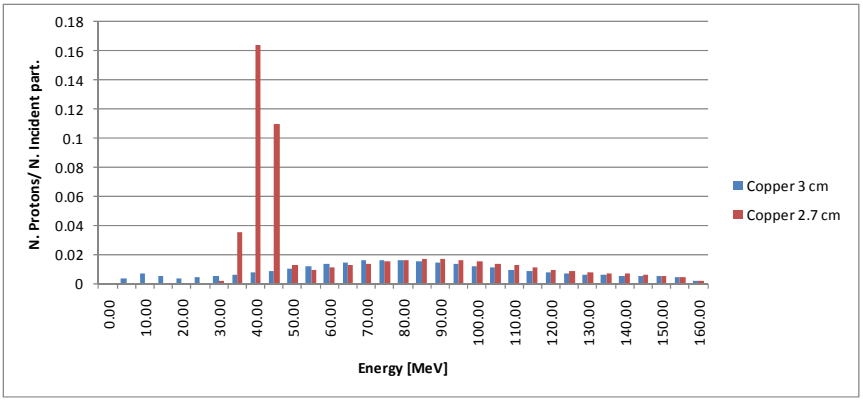

Figure 3.2.1 Proton energy distribution after the sieve. Copper

The energy distribution of H^- particles is the same for both cases. See Figure 3.2.2. As it was expected, the H^- that pass through the sieve holes without interact with the material keep their incident energy.

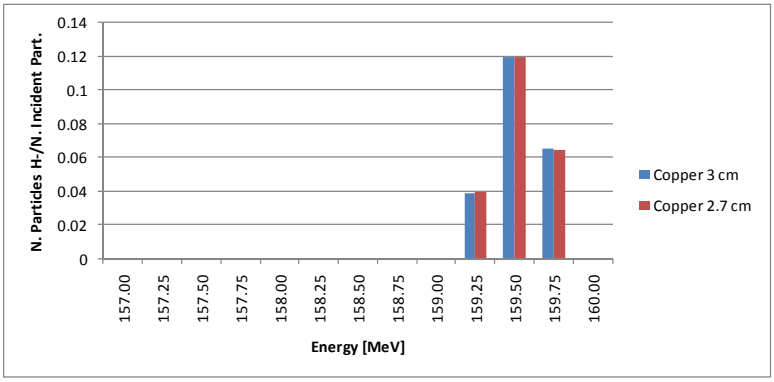

Figure 3.2.2 H^- energy distribution after the sieve. Copper

3.3.- Summary

The table below summarizes the distributions of the particles for the four study cases presented in this note, expressed in number of particles per primary (incident particle).

Material - Thickness	H- after the sieve per primary	Protons after the sieve per primary	Neutron after the sieve per primary	Total number of particles after the sieve per primary
Graphite - 10.5 cm	0.22	0.60	0.009	0.82
Graphite - 12 cm	0.22	0.35	0.009	0.58
Copper - 2.7 cm	0.22	0.57	0.014	0.80

Copper - 3 cm	0.22	0.29	0.014	0.52

4. Losses

PathManager simulation results for a through tracking of the protons and neutrons, from the sieve to the PSB, are presented in this section.

The part of the layout from the sieve to the end of the transfer line has been split in two conceptual parts to show the results in an efficient way. The first part goes from the starting point up to the septum and it is called common part, because the losses in this region can be considered independent of the destination of the H^- beam. In the second part of the line, downstream from SMV1 to the end of ring 3, different simulations have been performed to cover the four possible H^- beam destination.

4.1.- Graphite

The location and level of the losses in this layout is obtained tracking the graphite proton distribution, with a thickness of 10.5cm and 12 cm. (see section 3.1).

The following figure shows the proton losses in terms of watts along the first part of the line, assuming a 40 mA incident beam at 0.04% duty cycle.

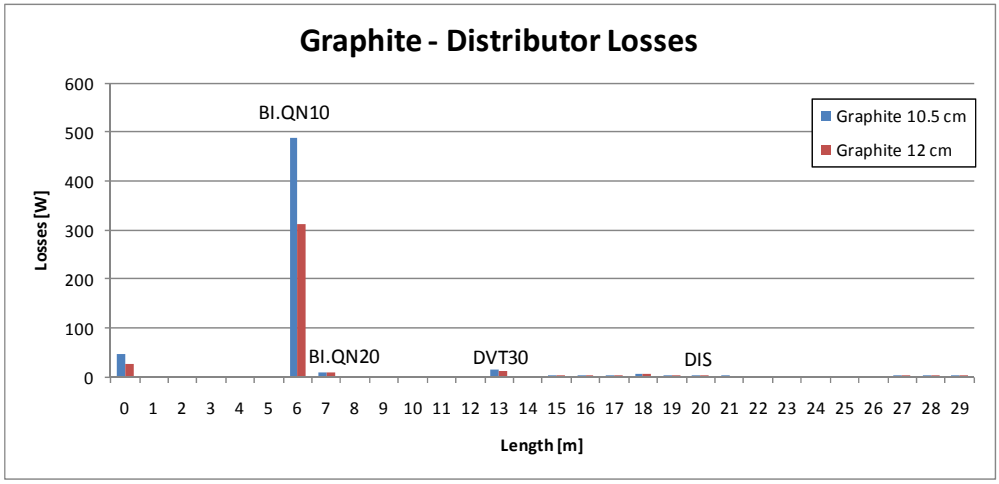

Figure 4.1.1 Proton Losses. Graphite.

Most of the proton losses are located in the first quadrupole BI.QN10.

Figure 4.1.2 shows the losses in the septum and along the line that leads the beam to PSB Ring3 for Graphite 10.5 cm. The integrated losses along the line for Graphite 10.5 cm in the worst case is **580 W.**

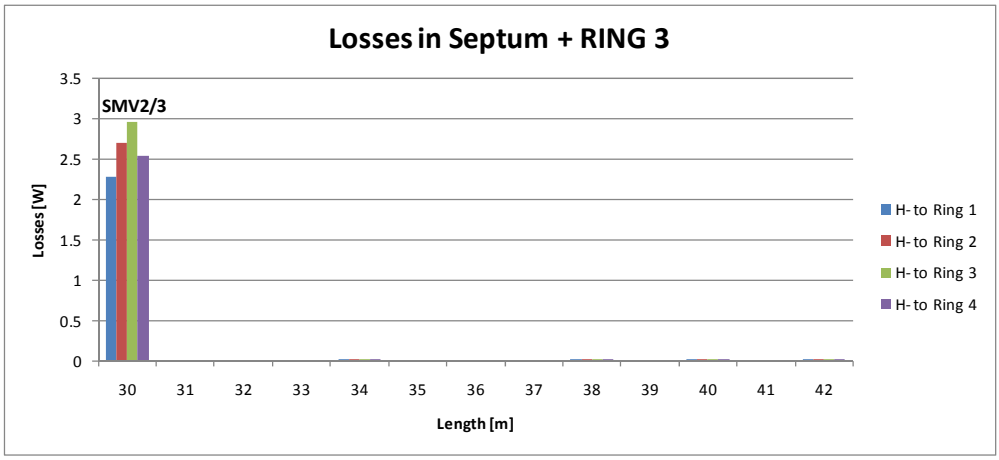

Figure 4.1.2 Proton Losses in the septum. Graphite 10.5 cm.

Figure 4.1.3 shows the losses in the septum and along the line that leads the beam to PSB Ring3 for Graphite 12 cm. The integrated losses along the line for Graphite 12 cm in the worst case is **380 W.**

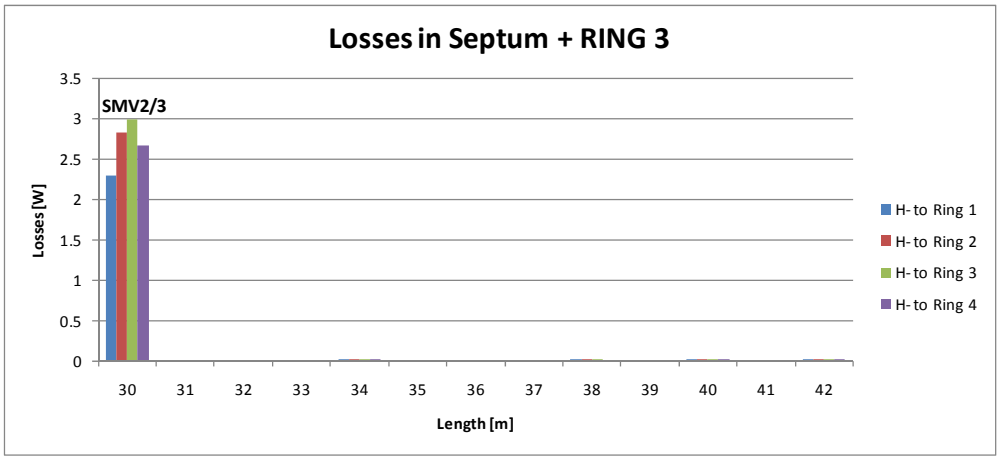

Figure 4.1.3 Proton Losses in the septum. Graphite 12 cm.

In both cases the level of the losses in the septum is similar, and the maximum power is originated when the H^- beam goes to the booster ring 3.

Neutrons generated in the sieve are also tracked, to detect where they hit the chamber. See Figure 4.1.4.

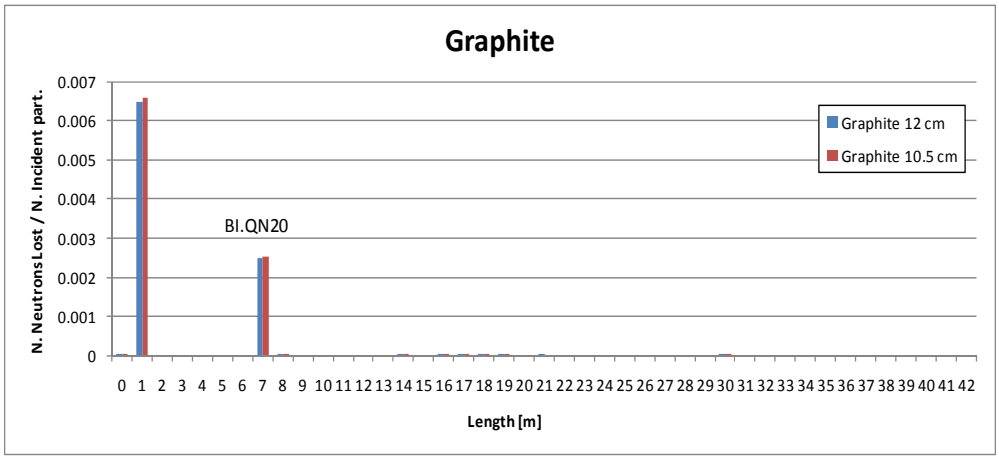

Figure 4.1.4 Number of neutrons lost normalized to the number of incident particles.

The transmission of protons to Booster ring 3 is summed up in the table below.

Destination H-	Graphite 10.5 cm ‰ Protons Output Ring 3	Graphite 12 cm ‰ Protons Output Ring 3
To Ring 1	0.16	0.30
To Ring 2	0.84	1.42
To Ring 3	0.89	1.65
To Ring 4	0.55	0.95

Table 4.1.1 Proton transmission to booster ring 3.

4.2.- Copper

Also the losses along the line have been studied tracking along the line the copper proton distribution, with a thickness value of 2.7 cm and 3 cm (see section 3.2).

The following figure shows the proton losses in terms of watts along the first part of the line, assuming a 40 mA incident beam at 0.04% duty cycle.

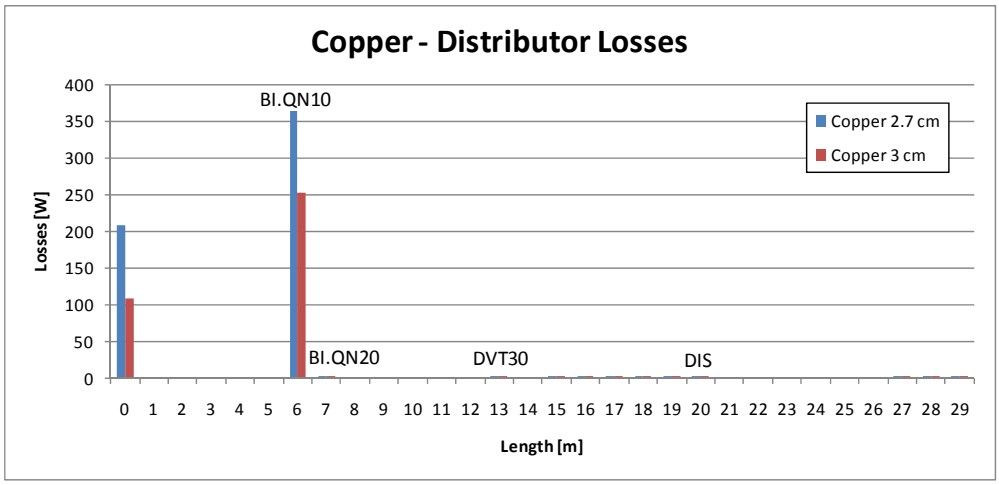

Figure 4.2.1 Proton Losses. Copper.

Most of the proton losses are located in the first quadrupole BI.QN10.

Figure 4.2.2 shows the losses in the septum and along the line that leads the beam to PSB Ring3, for a sieve made of copper, 2.7 cm thickness. The integrated losses along the line in the worst case is **576 W.**

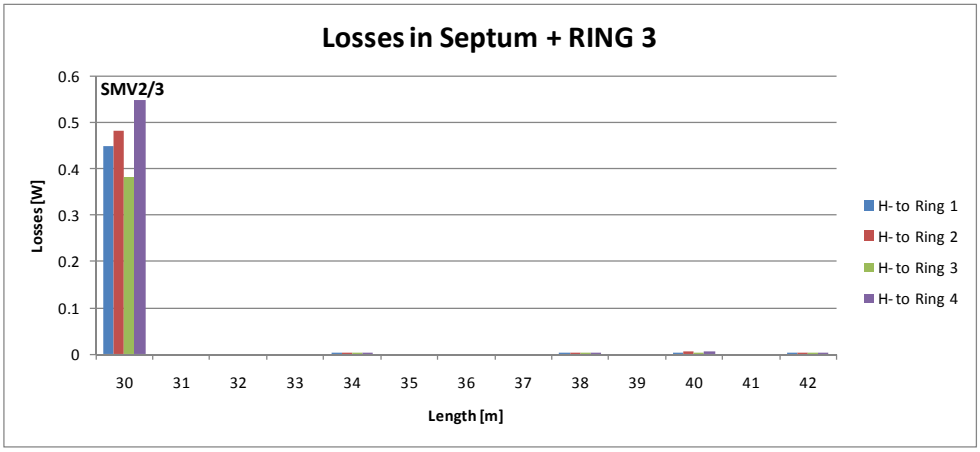

Figure 4.2.2 Proton Losses in the septum. Copper 2.7 cm.

Figure 4.2.3 shows the losses in the septum for a copper, 3cm thickness sieve. The integrated losses along the line in the worst case is **364 W.**

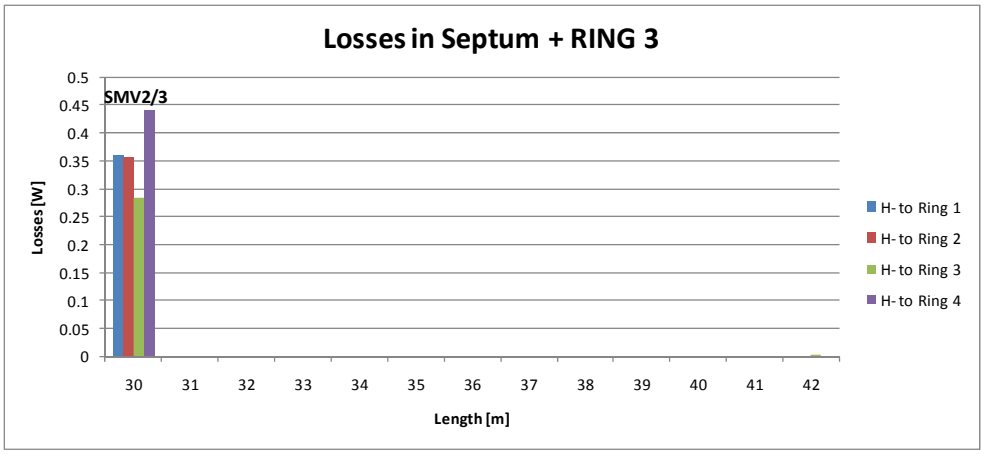

Figure 4.2.3 Proton Losses in the septum. Copper 3 cm.

Neutrons generated in the sieve are also tracked. See Figure 4.1.4.

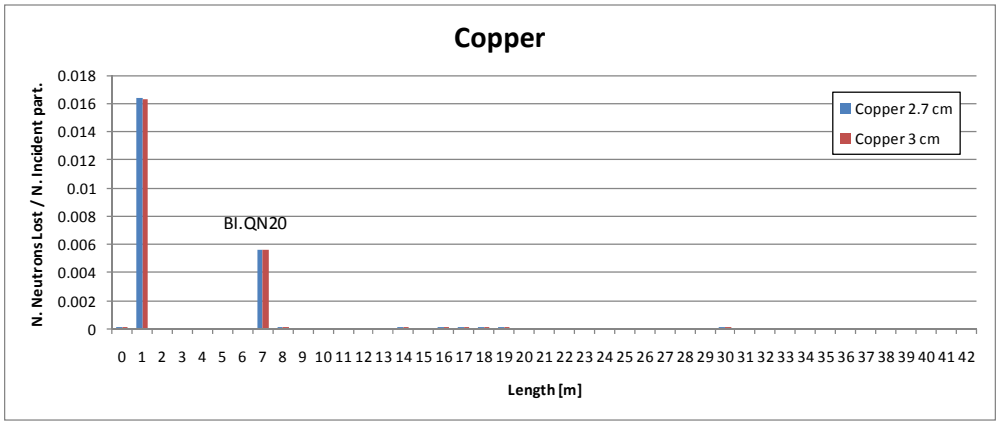

Figure 4.2.4 Number of neutrons lost normalized to the number of incident particles.

The transmission of protons to Booster Ring 3 is summed up in the table below. Maximum transmission occurs when the beam experiences the minimum bending (H^- to Ring 3).

Destination H-	Copper 2.7 cm %o Protons Output Ring 3	Copper 3 cm %o Protons Output Ring 3
To Ring 1	0.02	0.01
To Ring 2	0.09	0.19
To Ring 3	0.19	0.32
To Ring 4	0.04	0.07

Table 4.2.1 Proton transmission to booster ring 3.

5. Conclusions

In this note, different sieve materials and thicknesses have been studied in order to determine the level of the losses and their locations along the layout of the LINAC4 transfer line.

Only ~20% of H^- is stopped by the sieve for the thinner thicknesses in both materials. The rest come out as protons at degraded energy.

Most of the losses are located at the first two quads (QN10 and QN20). The level of losses is not acceptable. The limit of 1W/m is universally accepted for hands-on maintenance in linear accelerators [6]. Other locations of the sieve, at lower energy, are being considering (see APPENDIX A), as well as another approaches to reduce the intensity of the beam.

The distribution of the neutron losses is independent of the material thickness. No neutrons are transmitted to the PSB.

The thinner the sieve block, the higher the number of protons at degraded energy, which traverses the sieve and are lost in the line.

Protons arriving to septum magnets are lost; therefore there will be only protons at the end of ring 3.

6. References

[1] F. Gerigk, M. Vretenar editors, “LINAC4 Technical Design Report”, CERN-AB-2006-084 ABP/RF.

[2] A. Perrin and J.F Amand, Travel v4.07, users manual,CERN (2003).

[3] G. Bellodi, A.M. Lombardi, “Transfer Line Studies from LINAC4 to the PS Booster: Green Field Option”, CERN-AB-2007-037 ABP.

[4] "The FLUKA code: Description and benchmarking" G. Battistoni, S. Muraro, P.R. Sala, F. Cerutti, A. Ferrari, S. Roesler, A. Fasso`, J. Ranft, Proceedings of the Hadronic Shower Simulation Workshop 2006, Fermilab 6-8 September 2006, M. Albrow, R. Raja eds., AIP Conference Proceeding 896, 31-49, (2007)

[5] “FLUKA: a multi-particle transport code” A. Fasso`, A. Ferrari, J. Ranft, and P.R. Sala, CERN-2005-10 (2005), INFN/TC_05/11, SLAC-R-773

[6] N.V Mokhov and W.Chou editors, “Beam Halo and scraping”, Proc. 7th ICFA mini-workshop on high intensity and high brightness hadron beams, Interlaken resort, Wisconsin, United States, 1999

APPENDIX A: Alternative approaches to reduce the beam intensity.

New approaches changing the sieve location are being studied in order to solve the issues concerning the sieve at 160 MeV. Positioning the sieve at lower energy could potentially achieve the wanted reduction factor with much less power deposited in the sieve. Nevertheless the beam characteristics at the booster injection will not be as close to the nominal ones as with the sieve in the present position.

1.- Sieve at 50 MeV

A new study assuming the position of the sieve at 50 MeV (after the DTL) is presented below. A comparison between the parameters of the nominal beam, and the new low current beam (generated after the sieve), is shown in the following figures.

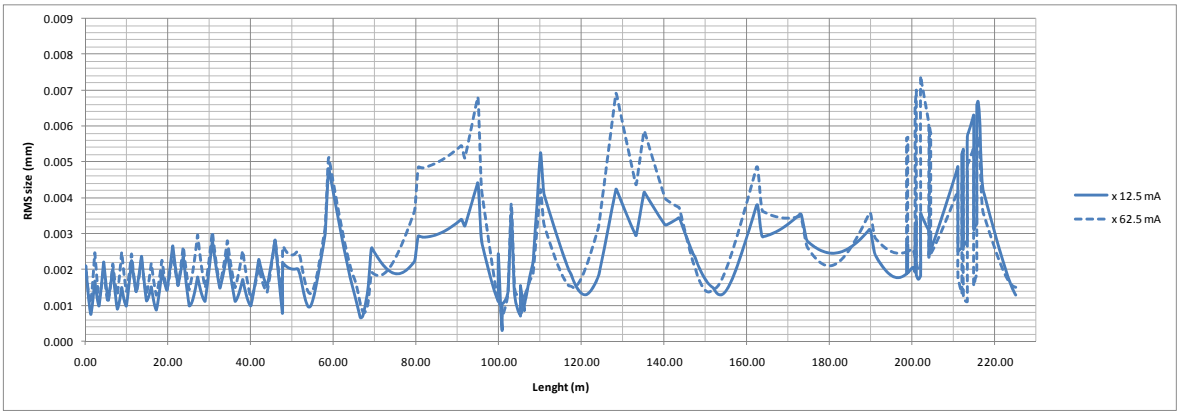

Figure 1.1.- Transverse (x) r.m.s envelope for the nominal current and the low current beam.

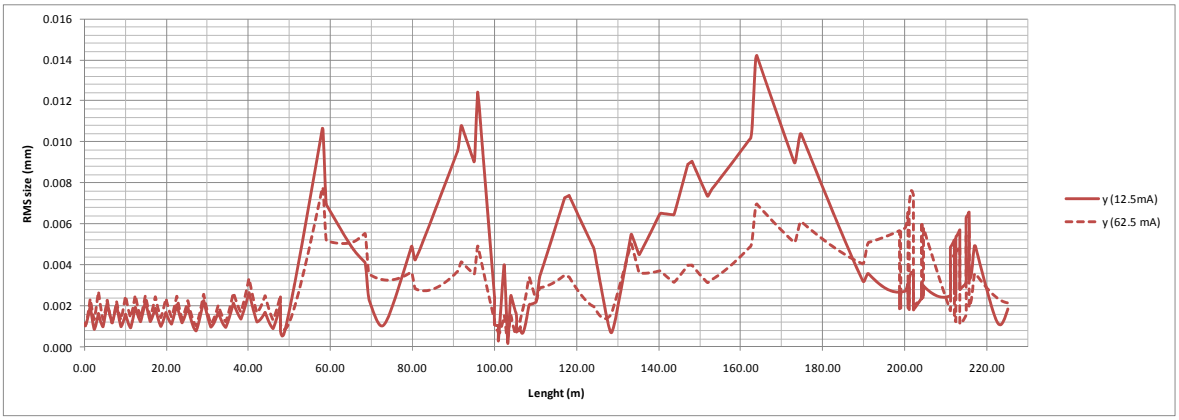

Figure 1.2.- Transverse (y) r.m.s envelope for the nominal current and the low current beam.

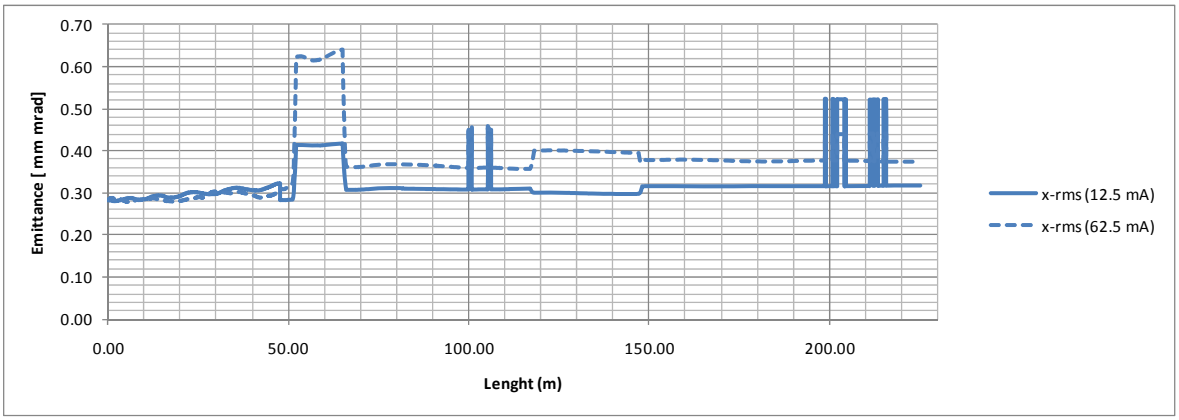

Figure 1.3.- Transverse r.m.s emittance (x).

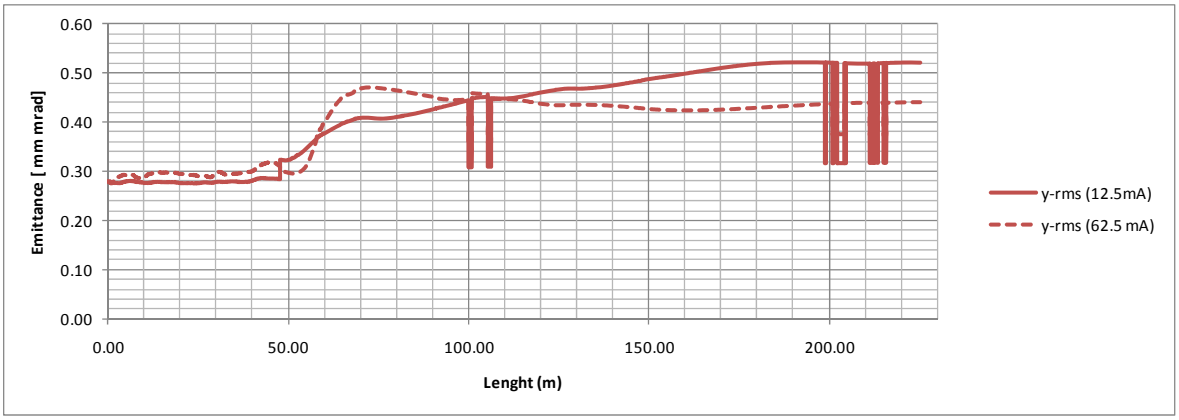

Figure 1.4.- Transverse r.m.s emittance (y).

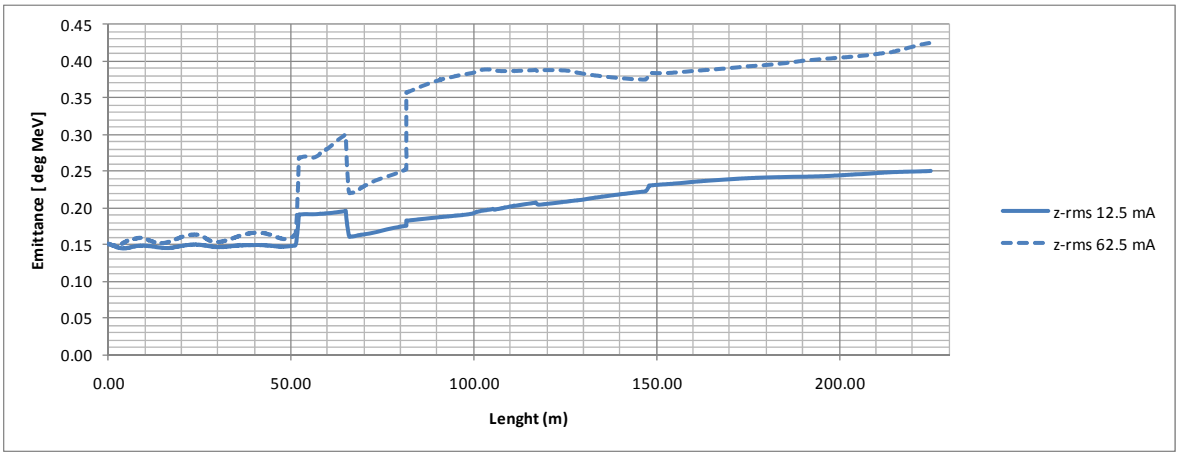

Figure 1.5.- Longitudinal r.m.s emittance (z).

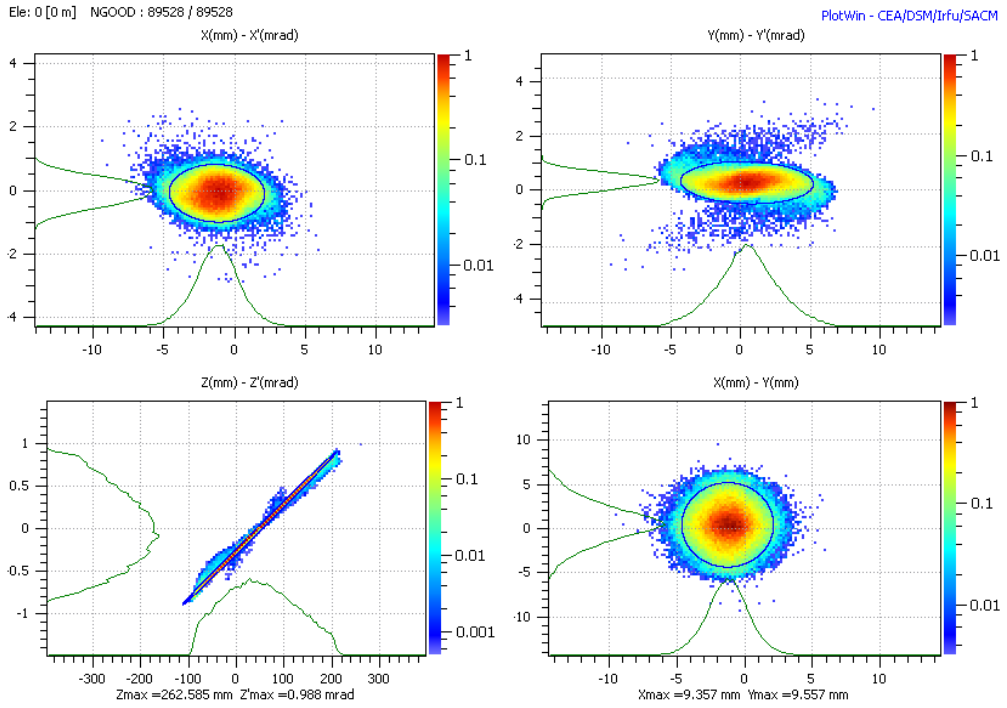

Figure 1.6.- Beam phase space at the output of the TL. Nominal current.

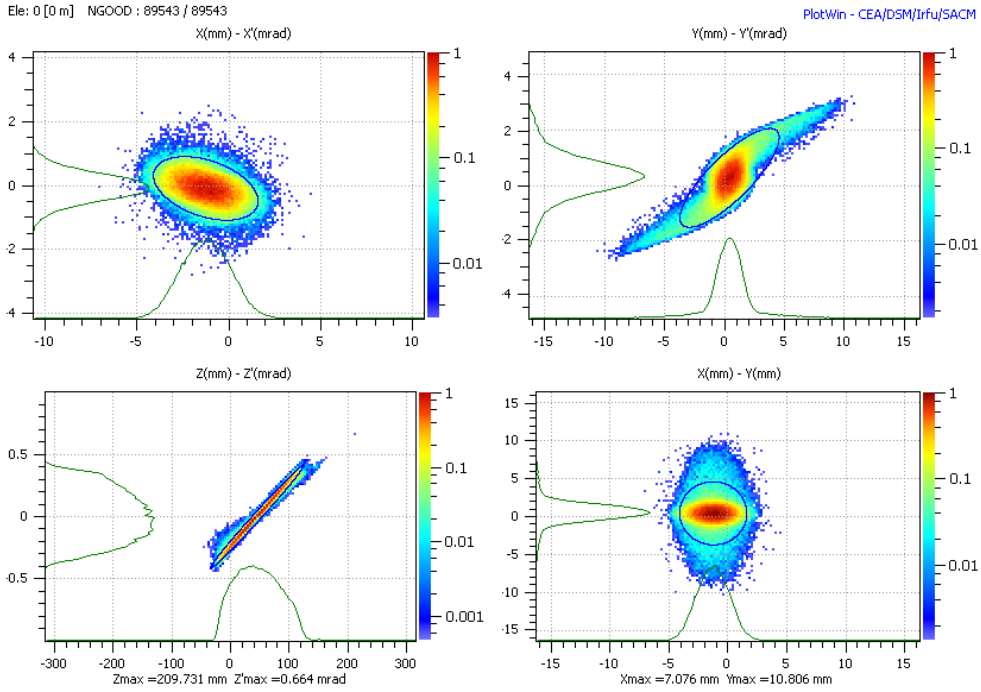

Figure 1.7.- Beam phase space at the output of the TL. (Using the sieve to reduce the current @50 MeV)

	Nominal current	Sieve current
(X,BGX') RMS-Emittance [m.rad]	3.73E-07	3.17E-07
(Y,BGY') RMS-Emittance [m.rad]	4.41E-07	5.22E-07
(PHI,dE) RMS-Emittance [deg.MeV]	4.25E-01	2.51E-01
(X,X') Alpha [1]	3.21E-02	4.38E-01
(X,X') Beta [m/rad]	3.73E+00	3.14E+00
(Y,Y') Alpha [1]	7.84E-02	-1.40E+00
(Y,Y') Beta [m/rad]	6.34E+00	3.99E+00
(PHI,dE) Alpha [1]	2.26E+01	8.83E+00
(PHI,dE) Beta [deg/MeV]	8.02E+03	3.37E+03

Table 1.1.- Parameters at the output of the TL for both cases.

2.- Sieve at 12 MeV

The same study assuming the position of the sieve at 12 MeV (after the first DTL tank) is presented below. A comparison between the parameters of the nominal beam, and the new low current beam (generated after the sieve), is shown in the following figures.

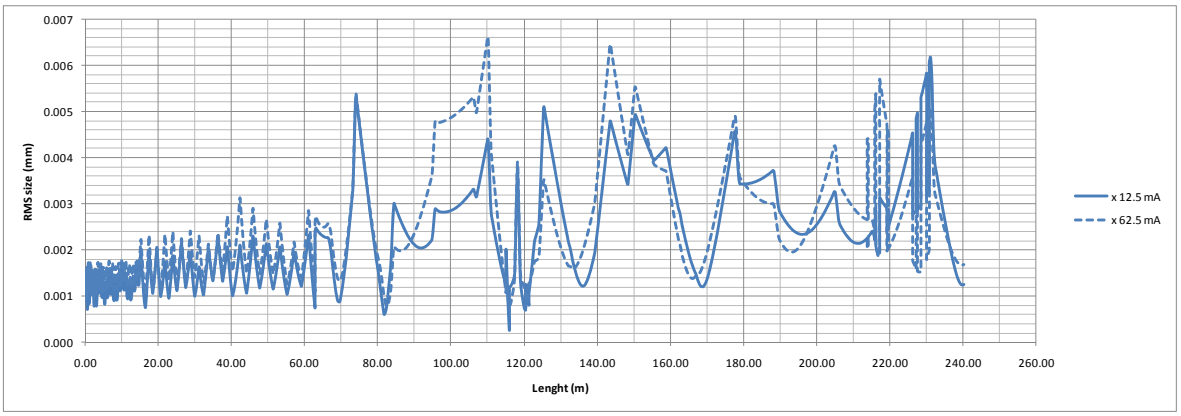

Figure 2.1.- Transverse (x) r.m.s envelope for the nominal current and the low current beam.

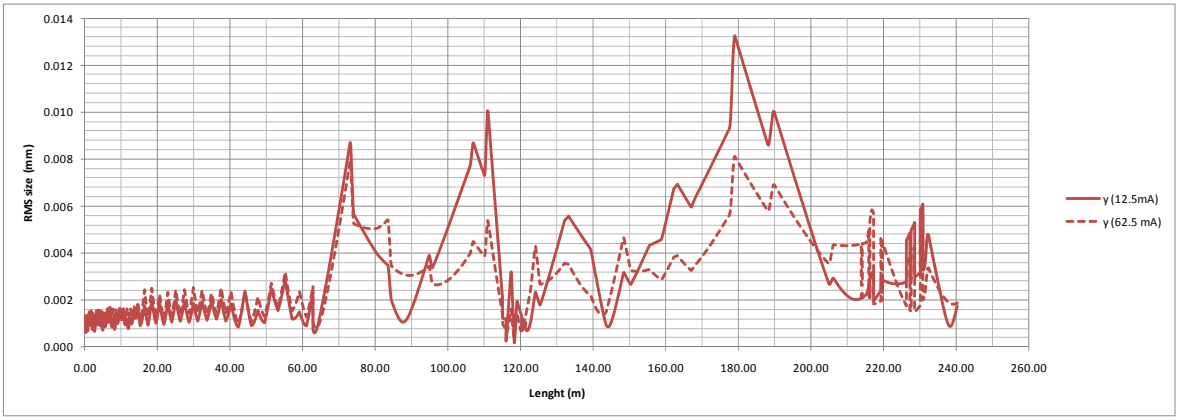

Figure 5.2.2.- Transverse (y) r.m.s envelope for the nominal current and the low current beam.

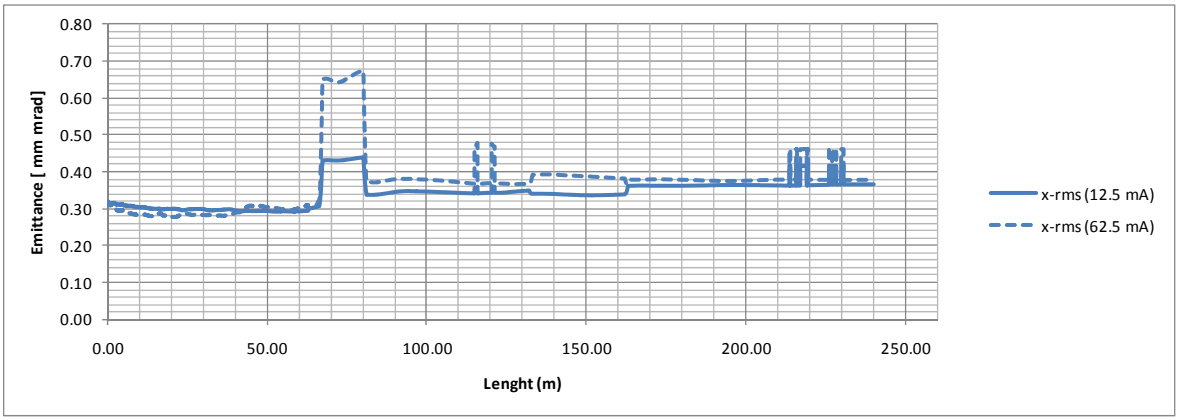

Figure 2.3.- Transverse r.m.s emittance (x).

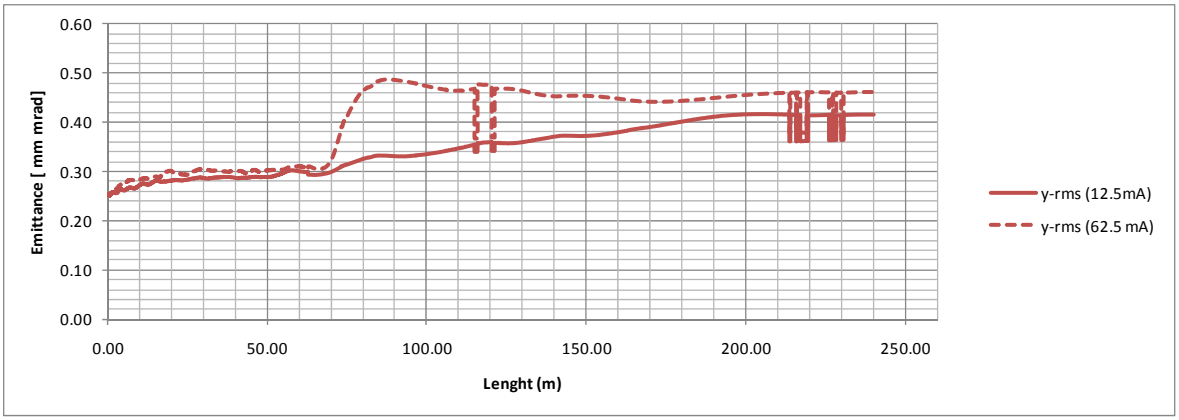

Figure 2.4.- Transverse r.m.s emittance (y).

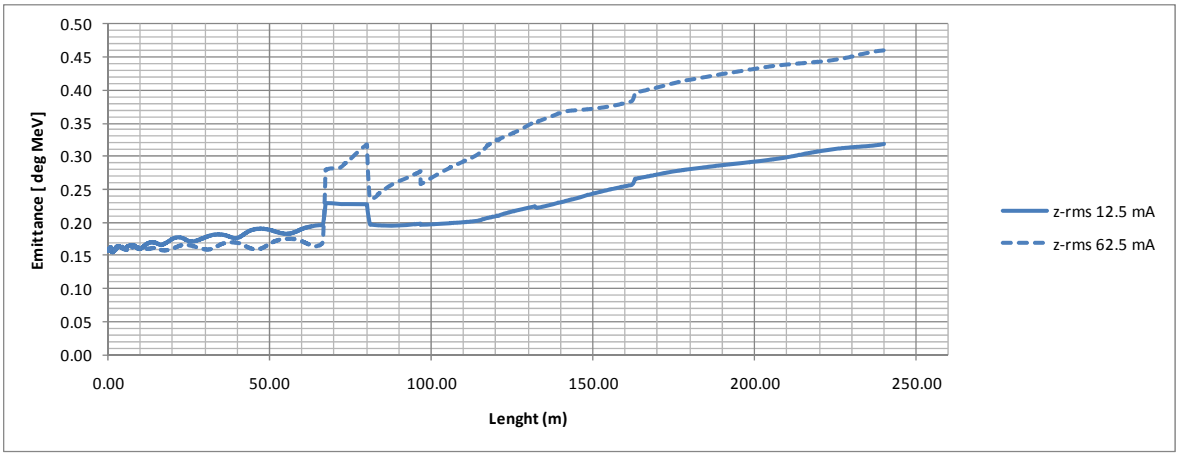

Figure 2.5.- Longitudinal r.m.s emittance (z).

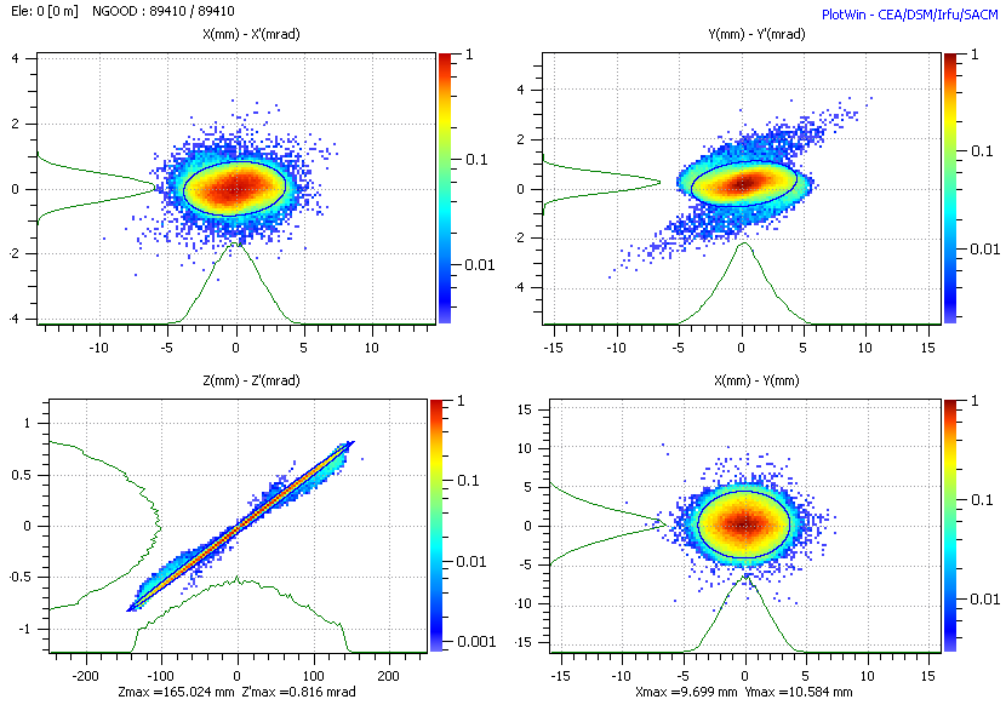

Figure 2.6.- Beam phase space at the output of the TL. Nominal current.

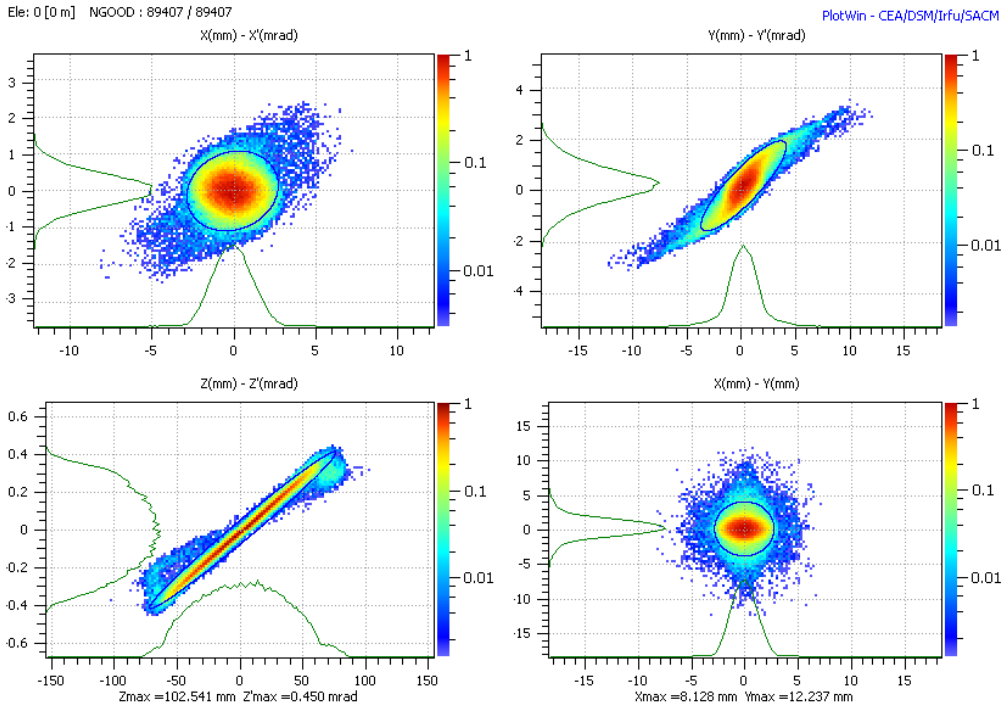

Figure 2.7.- Beam phase space at the output of the TL. Sieve current.

	Nominal current	Sieve Current
(X,BGX') RMS-Emittance [m.rad]	3.77E-07	3.65E-07
(Y,BGY') RMS-Emittance [m.rad]	4.61E-07	4.17E-07
(PHI,dE) RMS-Emittance [deg.MeV]	4.61E-01	3.19E-01
(X,X') Alpha [1]	-1.17E-01	-1.44E-01
(X,X') Beta [m/rad]	4.56E+00	2.62E+00
(Y,Y') Alpha [1]	-2.38E-01	-1.75E+00
(Y,Y') Beta [m/rad]	4.72E+00	4.51E+00
(PHI,dE) Alpha [1]	1.78E+01	6.41E+00
(PHI,dE) Beta [deg/MeV]	6.39E+03	2.28E+03

Table 2.1.- Parameters at the output of the TL for both cases.

3.- Sieve at 3 MeV

Simulations assuming the position of the sieve at 3 MeV (before the DTL) is presented below. A comparison between the parameters of the nominal beam, and the new low current beam (generated after the sieve), is shown in the following figures.

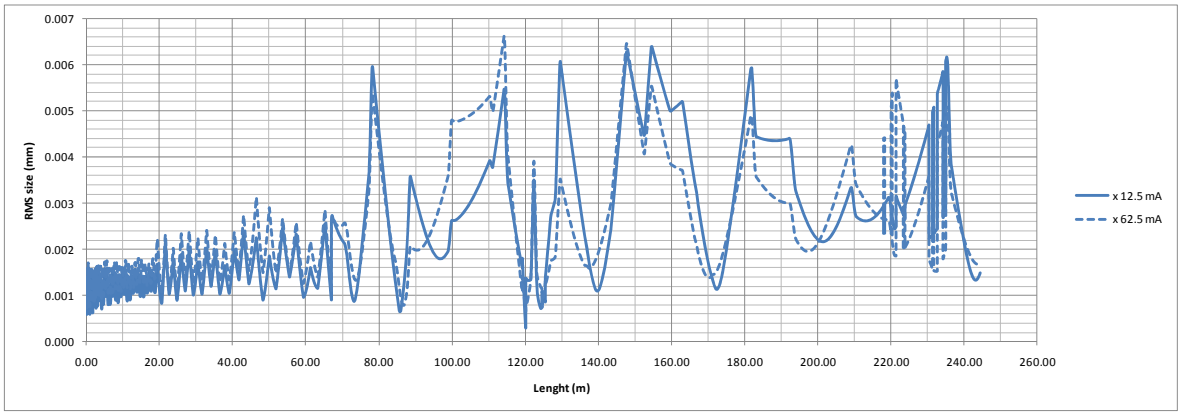

Figure 3.1.- Transverse (x) r.m.s envelope for the nominal current and the low current beam.

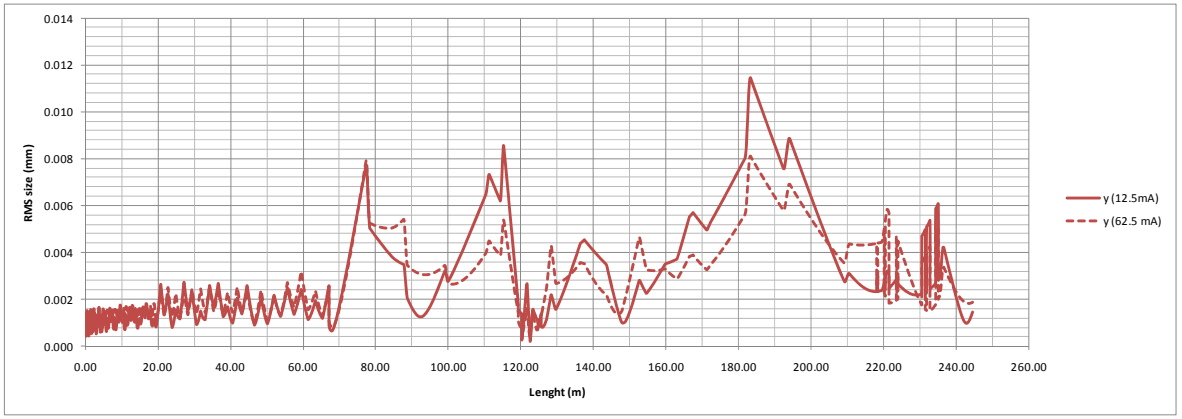

Figure 3.2.- Transverse (y) r.m.s envelope for the nominal current and the low current beam.

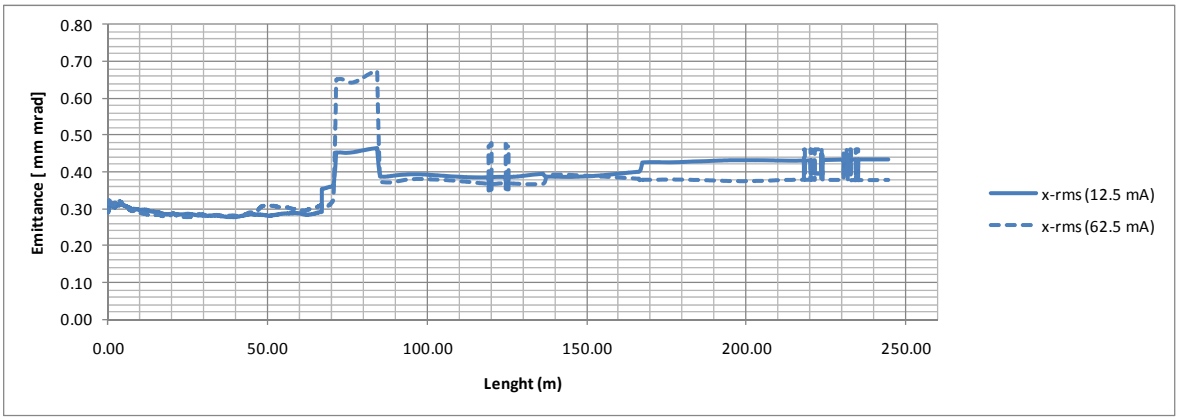

Figure 3.3.- Transverse r.m.s emittance (x).

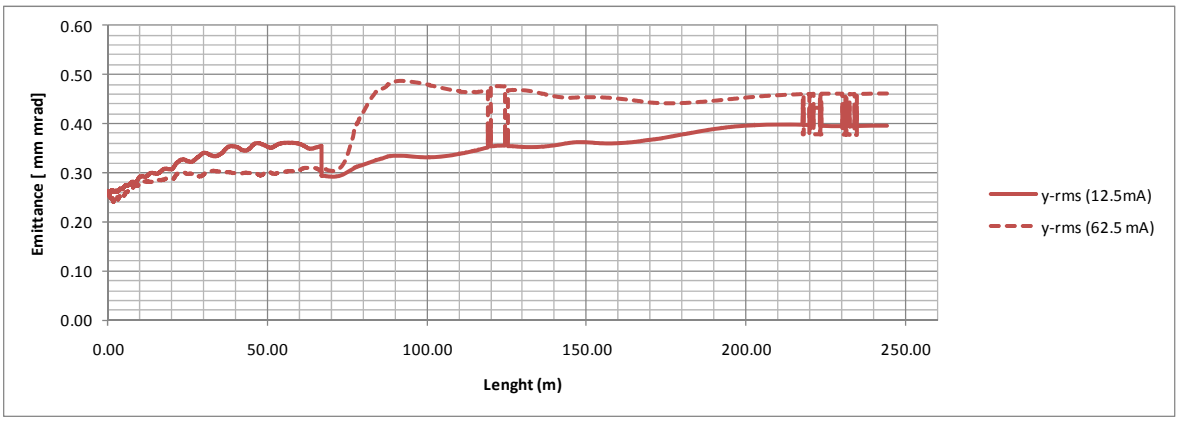

Figure 3.4.- Transverse r.m.s emittance (y).

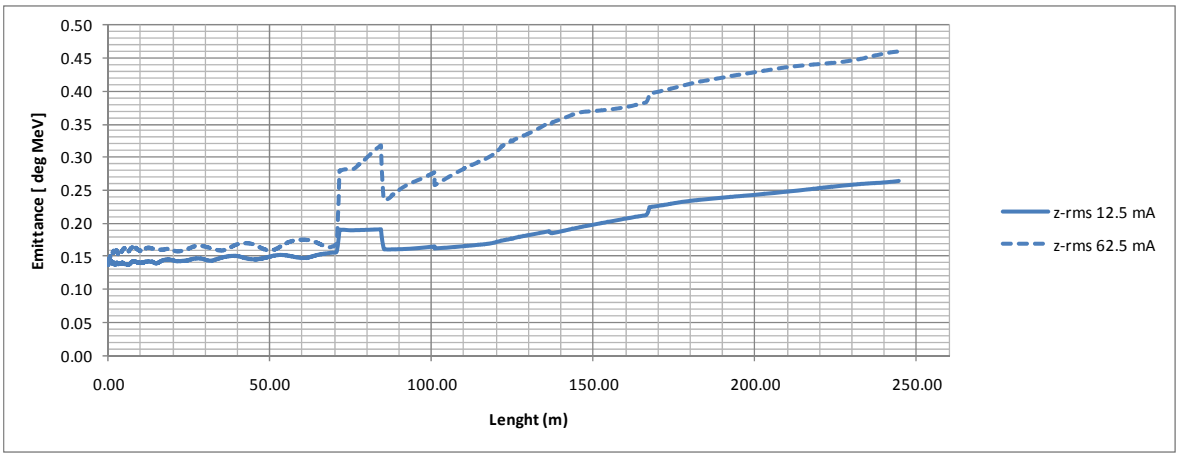

Figure 3.5.- Longitudinal r.m.s emittance (z).

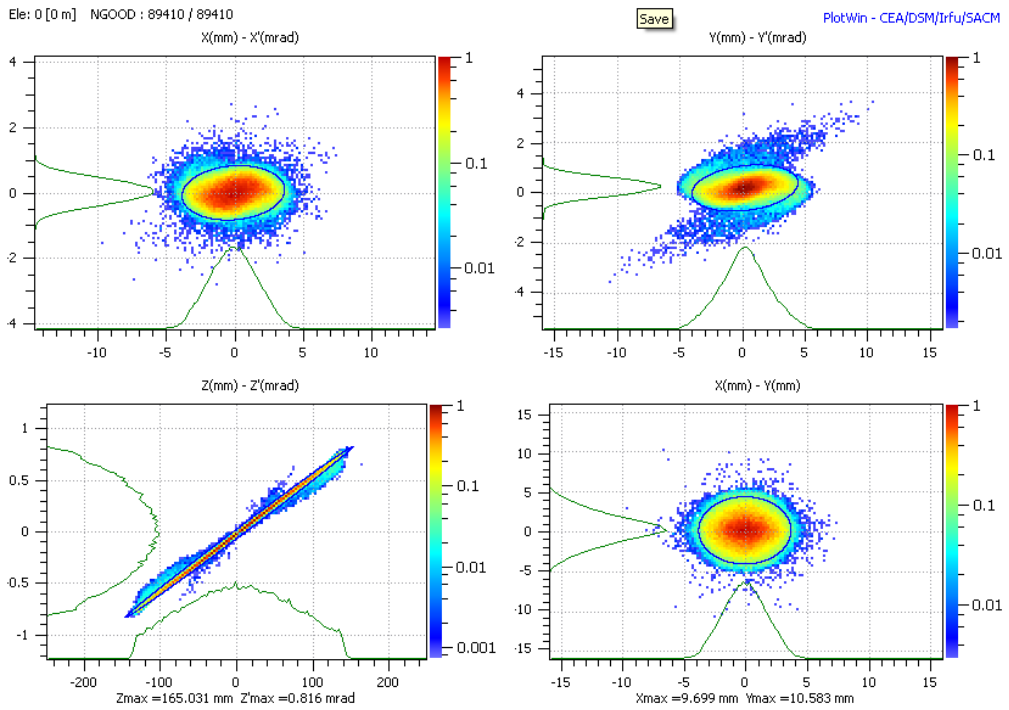

Figure 3.6.- Beam phase space at the output of the TL. Nominal current.

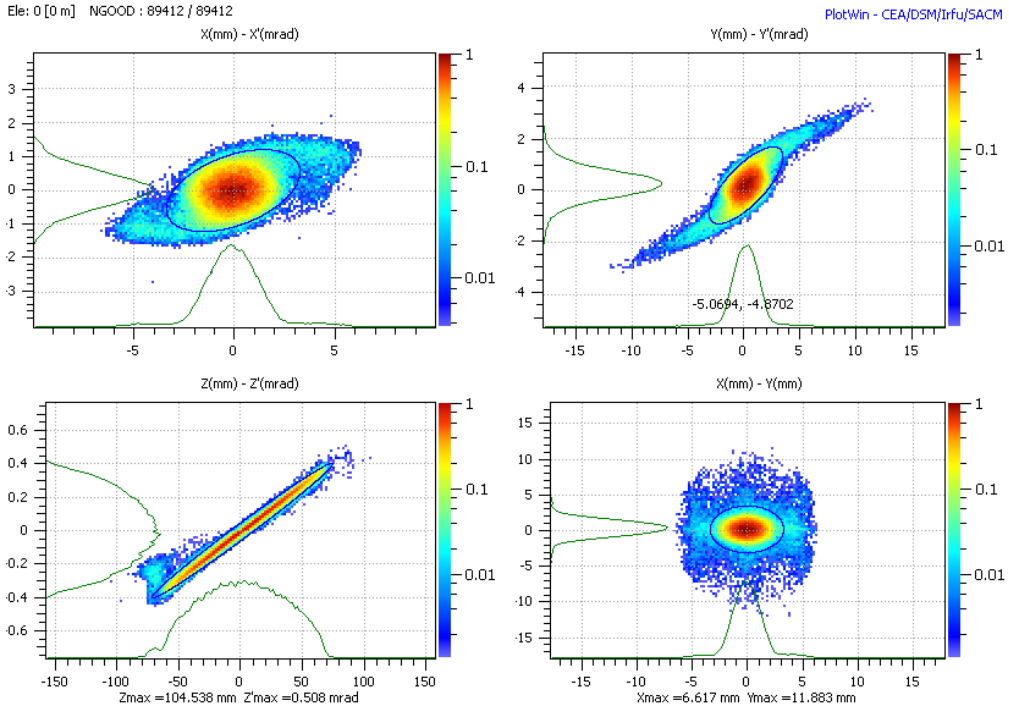

Figure 3.7.- Beam phase space at the output of the TL.Sieve current.

	Nominal current	Sieve Current
(X,BGX') RMS-Emittance [m.rad]	3.77E-07	4.34E-07
(Y,BGY') RMS-Emittance [m.rad]	4.61E-07	3.96E-07
(PHI,dE) RMS-Emittance [deg.MeV]	4.61E-01	2.63E-01
(X,X') Alpha [1]	-1.16E-01	-5.03E-01
(X,X') Beta [m/rad]	4.56E+00	3.10E+00
(Y,Y') Alpha [1]	-2.38E-01	-1.10E+00
(Y,Y') Beta [m/rad]	4.72E+00	3.34E+00
(PHI,dE) Alpha [1]	1.78E+01	7.46E+00
(PHI,dE) Beta [deg/MeV]	6.39E+03	2.70E+03

Table 3.1.- Parameters at the output of the TL for both cases.